Interaction Between Coxsackievirus B3 Infection and α-Synuclein in Parkinson's Disease

Soo Jin Park
Ajou University School of Medicine and Graduate School of Medicine
Uram Jin
Ajou University School of Medicine and Graduate School of Medicine
Sang Myun Park (sangmyun@ajou.ac.kr)
Ajou University School of Medicine https://orcid.org/0000-0002-1001-4743

Research article

Keywords: Parkinson's disease, α-synuclein, Lewy body, coxsackievirus

Posted Date: January 19th, 2021

DOI: https://doi.org/10.21203/rs.3.rs-145815/v1

Abstract

Background

Parkinson's disease (PD) is one of the most common neurodegenerative disease. PD is pathologically characterized by the death of midbrain dopaminergic neurons and the accumulation of intracellular protein inclusions called Lewy bodies or Lewy neurites. The major component of Lewy bodies is α-synuclein (α-syn). Prion-like propagation of α-syn has emerged as a novel mechanism in the progression of PD. Targeting this mechanism could enable the development of disease-modifying therapies for patients with PD. Nevertheless, the initial triggers of LB formation leading to acceleration of the process remain elusive.

Methods

To evaluate α-syn function in viral replication, we infected coxsackievirus B3 (CVB3) to α-syn overexpressed neurons or α-syn transgenic (TG) mice. We then performed biochemical and histological analyses to evaluate interaction between CVB3 and α-syn in Lewy body formation.

Results

We demonstrated that CVB3 infection can induce α-syn-associated inclusion body formation in neurons as a trigger. The inclusion bodies contained clustered organelles, including damaged mitochondria with α-syn fibrils. α-Syn overexpression accelerated inclusion body formation and induced more concentric inclusion bodies. In brains from CVB3 infected mice, α-syn aggregates in the cell body of midbrain neurons were observed. Additionally, α-syn overexpression favored CVB3 replication and related cytotoxicity. α-Syn transgenic mice had a low survival rate, enhanced CVB3 replication, and further neuronal cell death, including dopaminergic neurons in the substantia nigra. These results may be due to the different usage of autophagy between CVB3 and α-syn.

Conclusions

This study elucidated the mechanism of Lewy body formation and the pathogenesis of PD associated with CVB3 infection.

Background

Parkinson's disease (PD) is one of the most common neurodegenerative disease. PD is pathologically characterized by the death of midbrain dopaminergic neurons and the accumulation of intracellular protein inclusions termed Lewy bodies (LBs) or Lewy neurites (LNs) [1, 2]. The major component of these inclusions is α-synuclein (α-syn) [3]. Protein inclusions with α-syn aggregates have also been observed in other neurodegenerative disorders, such as multiple system atrophy and dementia with Lewy body, which are collectively referred to as α-synucleinopathies [4]. Multiplications and missense mutations of the α-syn gene have been identified in patients with early onset familial PD [5]. Genome-wide association

studies also demonstrated a strong association between α-syn gene and sporadic PD [6, 7], suggesting a major role of α-syn in the pathogenesis of PD.

Lewy pathology first appears in the olfactory bulbs and dorsal motor nucleus of the vagus nerve, which is connected to the enteric nervous system. The pathology progressively involves more regions of the nervous system and then the cortical areas as the disease advances [8]. This pathology seems to be present prior to the appearance of motor symptoms in PD and may be associated with gastrointestinal and olfactory dysfunctions, which are frequently present in the prodromal phase of PD [9]. Substantial *in vitro* and *in vivo* experimental evidence has implicated the prion-like propagation of α-syn as a novel mechanism in the progression of PD [10–12]. Targeting this mechanism could enable the development of disease-modifying therapies for patients with PD. Hampering this aim, the initial triggers of LB formation leading to acceleration of the process remain elusive.

Viral infection is increasingly recognized as a risk factor for PD. A number of viruses have been associated with both acute and chronic parkinsonism. These viruses include influenza virus, coxsackievirus, Japanese encephalitis B virus, western equine encephalitis virus, and herpes virus [13]. It has been proposed that peripheral infections, including viral infections accompanying inflammation, may trigger PD [14].

Coxsackievirus is a single-stranded RNA virus belonging to the *Picornaviridae* family of viruses in the genus termed *Enterovirus* [15]. More than 90% of coxsackieviruses infections are asymptomatic. Clinically, infants or young adults are easily infected with this virus, and a small number develop severe myocarditis [16] or meningitis [17]. Persistent coxsackievirus infection is also associated with chronic myocarditis, dilated cardiomyopathy [18], and type I diabetes [19].

A recent report described virus-like particles and enterovirus antigen in the brainstem neurons of PD [20]. This finding prompted the proposal that enterovirus infection in PD may act as a seed for the aggregation of α-syn in addition to the direct cytopathic effect of a virus infection on neurons. In addition, α-syn inhibits West Nile virus (WNV) infection as a viral restriction factor [21], suggesting that α-syn expression may affect viral infection in the central nervous system (CNS).

In the present study, we explored whether coxsackievirus B3 (CVB3) interacts with α-syn to induce aggregation and further LB formation, and whether α-syn affects the replication of coxsackievirus.

Methods

Antibodies and reagents

Antibodies against α-syn were purchased from Abcam (#ab138501, Cambridge, UK), BD Biosciences (#610786, Franklin Lakes, NJ), and Genetex (#GTX112799, Santa Barbara, CA). Antibodies against pSer129 α-syn (#ab51253) and Tuj-1 (#ab18207) were obtained from Abcam. Antibody against VP1 of CVB3 was purchased from Millipore (#MAB948, Danvers, MA). Antibody against LC3 was purchased

from Sigma-Aldrich (#L8918, St. Louis, MO). Antibody against p62 was purchased from BD Biosciences (#610832). Antibody against cleaved caspase-3 was purchased from Cell Signaling Technology (#9664, Beverly, MA). Antibody against IBA-1 was purchased from Wako (#019-19741, Richmond, VA). Antibody against glial fibrillary acidic protein (GFAP) was purchased from Neuromics (#RA22101, Montreal, QC). Antibody against glyceraldehyde 3-phosphate dehydrogenase (GAPDH) was purchased from Santa Cruz Biotechnology (#SC-32233, Santa Cruz, CA). LysoTracker (#L12492) and Lipofectamine2000 (#11668-019) were obtained from Invitrogen (Carlsbad, CA). Retinoic acid (RA, #r2625), Bafilomycin A1 (Baf A1, #B1793), polyinosine:polycytidylic acid (poly IC, #P0913), and Evans Blue Dye (EBD, #E2129) were purchased from Sigma-Aldrich. Sudan Black B was purchased from Tokyo Chemical Industry (#4197 – 2505, Tokyo, Japan).

Animals

α-Syn transgenic (TG) mice overexpressing human α-syn under the control of neuron specific enolase (NSE) promotor (C57BL/6N-Tg (NSE-h a Syn) Korl) were donated by the National Institute of Food and Drug Safety Evaluation (NIFDS, Cheongju, Korea). Wild-type (WT) littermates or WT C57Bl/6N mice (DBL, Eumseong, Korea) were used as controls. All animal procedures were conducted according to the guidelines established by the Ajou University School of Medicine Ethics Review Committee (IACUC No. 2016-0047).

Cell culture

α-Syn, mCherry and α-syn-mCherry overexpressing SH-SY5Y cells were prepared as described previously [22]. The cells were grown in Dulbecco's modified Eagle's medium (DMEM) containing 10% fetal bovine serum (FBS) at 37 °C in a humidified atmosphere of 5% CO_2 and 95% air. Primary cortical neurons were cultured from 1-day-old pups of WT and α-syn TG mice in neurobasal medium (#21103-049, Invitrogen) with GlutaMAX^{TM}-I (#35050061, Thermo Fisher Scientific, Waltham, MA), and B-27 supplement (#17504-044, Invitrogen) for 2 weeks on poly-D-lysine (#P7280, Sigma-Aldrich) coated cover-slides or cell culture dishes. To differentiate SH-SY5Y cells, 50 μM of RA was added to the culture medium and incubated for 5 days.

Infection with coxsackievirus B3 (CVB3)

The H3 variant of CVB3, the Woodruff strain, and EGFP-CVB3 were a kind gift from Dr. E. Jeon (Samsung Medical Center, Seoul, Korea). The virus was propagated in HeLa cells. Viral titers were determined using plaque forming assay. SH-SY5Y cells were incubated with CVB3 at an indicated multiplicity of infection (MOI) in serum-free DMEM for 1 h and further incubated in DMEM with 10% FBS for 24 h. For primary neurons, cells were incubated with the indicated MOI of CVB3 in neuron culture medium for 24 h. In the *in vivo* model, 8- to 11- week-old male mice were infected by intraperitoneal (IP) injection with 1.0 x 10^6 plaque forming units (PFU) of CVB3 in 100 μl of phosphate-buffered saline (PBS).

Tissue preparation

Mice were anesthetized and transcardially perfused first with perfusion solution containing 0.5% sodium nitrate and 10 U/ml heparin, and then with 4% paraformaldehyde in 0.1 M phosphate buffer (PB; pH 7.2). Brains were stored in 4% paraformaldehyde for 24 h at 4 °C, and then in a 30% sucrose solution until they sank. For reverse transcription polymerase chain reaction (RT-PCR) and western blotting, mice were perfused with only perfusion solution for 2 min and each organ was stored at − 70 °C until use. For immunostaining, six separate series of 30 μm coronal brain sections were sectioned using a model CM3050S cryostat (Leica, Wetzlar, Germany) and stored in an anti-freeze stock solution (PB containing 30% glycerol and 30% ethylene glycol, pH 7.2) at 4 °C before experiments.

Immunocytochemistry

Cells cultured on coverslips were washed three times with PBS and fixed with 4% paraformaldehyde for 10 min at room temperature. The fixed cells were washed several times with PBS and incubated in the presence of permeabilization buffer (PBS containing 0.1% Triton X-100) for 5 min at room temperature. After washing with PBS, the cells were blocked with blocking buffer (PBS containing 1% bovine serum albumin [BSA]) for 1 h at room temperature, and then incubated with the indicated antibodies overnight at 4 °C. The samples were then incubated with Alexa 488- (#A21202, #A21206) or 568- (#A10037, #A10042) conjugated secondary antibodies (all from Invitrogen) for 1 h and then exposed to Hoechst stain for 5 min. The sections were mounted and observed by confocal microscopy (Carl Zeiss, Jena, Germany). Live cells were incubated with 50 nM LysoTracker in DMEM with 10% FBS for 30 min. After staining of nuclei with Hoechst for 5 min, the live cells were observed by confocal microscopy (Carl Zeiss).

Western blot

Samples were lysed in an ice-cold RIPA buffer (50 mM Tris-HCl, pH 7.4, 0.5% sodium deoxycholate, 150 mM NaCl, 0.1% SDS, 1% Triton X-100) containing a protease inhibitor cocktail (#535140, Calbiochem, Darmstadt, Germany) and a phosphatase inhibitor cocktail (#P3200-001, GenDEPOT, Baker, TX). After brief sonication, the lysates were centrifuged at 16,000 x g for 30 min at 4 °C, and the supernatants were collected. In case of mice tissues (brains and hearts), after lysing and homogenizing samples with TRIzol (#TR118, Molecular Research Center Inc, Cincinnati, OH, USA), protein was isolated according to the manufacturer's protocol. The protein concentrations were determined using a DC Protein Assay Reagents Package (#5000116, Bio-Rad, Hercules, CA). Proteins were resolved by SDS-PAGE, transferred to a PVDF or NC membrane, and immunoblotted with the indicated primary antibodies and horseradish peroxidase-conjugated secondary antibody (#G-21040, Invitrogen or #111-035-003, Jackson ImmunoResearch, West Grove, PA). They were then visualized using an enhanced chemiluminescence (ECL) system (#LF-QC0101, AbFrontier, Seoul, Korea). The band intensities were determined using ImageJ software (NIH, Bethesda, MD).

RT-PCR

Total RNA was isolated from samples using TRIzol (#TR118, Molecular Research Center Inc.) according to the manufacturer's protocol. Total RNA was reverse transcribed using AMV Reverse Transcriptase (#M0277L, New England Biolabs, Ipswich, MA). The transcript levels of target genes were quantified with 2×KAPA SYBR Fast Master Mix (#kk4602, Kapa Biosystems, Cape Town, South Africa) using the StepOnePlus™ Real-Time PCR System (Applied Biosystems, Foster City, CA). For each target gene, the transcript level was normalized to that of GAPDH and was calculated using the standard ΔΔCT method. A complete list of primer sequences is provided in Supplementary Table 1.

Transmission electron microscopy (TEM)

Control and CVB3 infected samples were fixed with 0.1M sodium cacodylate buffer (pH 7.4) containing 1% formaldehyde / 2% glutaraldehyde for 30 min at 4 °C [23]. The samples were rinsed twice with cold PBS, post-fixed with a mixture of 1% osmium tetroxide and 1% potassium ferricyanide, dehydrated in graded alcohol and embedded in Durcupan ACM resin (Fluka, Yongin, Korea). Ultrathin sections were obtained with resin, mounted on copper grids, and counterstained with uranyl acetate and lead citrate. The specimens were observed using a Sigma 500 transmission electron microscope (Carl Zeiss).

Mitochondrial morphology analysis

Mitochondrial morphology in TEM images was analyzed as described previously [24]. Based on the type of mitochondrial restructuring, four categories (type I-IV) were assigned. Type I comprised mitochondrial cristae that were regular, tightly packed, and longitudinally oriented. Type II comprised mitochondria with an abnormal shape or nonuniform size, and irregular cristae that lacked orientation and tightness. Type III comprised mitochondria of varied shapes and sizes, with discontinuous outer membrane, fragmented cristae, and swollen matrix. Type IV comprised mitochondria with a ruptured outer membrane, no cristae, and myelin-like transformation.

Cytotoxicity assay

Cytotoxicity assays were performed using the LDH Cytotoxicity Assay Kit (#K311-400, BioVision; Mountain View, CA) according to the manufacturer's protocol. Following the CVB3 infection for 30 h, 50 µl of medium and assay kit solution were mixed in wells of an optically clear 96-well plate. The absorbance was measured within 10 min at 490 nm with an ELISA reader (Molecular Device, Wokingham, UK)

Flow cytometry

Flow cytometry analysis was performed as described previously [25]. After the indicated times of EGFP-CVB3 infection, the cells were isolated and fixed by resuspension in 4% paraformaldehyde in PBS overnight. After washing with PBS and resuspension in 1% BSA in PBS, the cells were analyzed using a FACS Aria III (BD, Franklin Lakes, NJ). The data were analyzed using Flowing Software version 2.5.1 (Turku Bioscience, Turku, Finland).

Immunohistochemistry (IHC)

Every serial section in each set was collected and washed with PBS containing 0.2% Triton X-100 (PBST). After blocking with 1% BSA in PBST, sections were incubated overnight at room temperature with the indicated primary antibodies. The samples were incubated with Alexa 488- (#A21202, #A21206) or 568- (#A10037, #A10042) conjugated secondary antibodies (all from Invitrogen) for 1 h and then stained using Hoechst for 10 min. After mounting on slides, the sections were treated with Sudan Black B solution (0.1% in 70% ethanol) to inhibit auto-fluorescence of mouse tissues. Images were captured using a confocal microscope (Carl Zeiss) or a fluorescence microscope (Axioscan Z1, Carl Zeiss).

Cell density analysis

The hemispheres of mice were used for detecting VP1 by RT-PCR. The opposite hemispheres were used to analyze cell density. The hemispheres from three mice whose brain VP1 levels were close to the average were analyzed. We measured the number of cells (neurons) and the density of cells (microglia) per specific anatomical structure. Tuj-1 merged VP1 positive cells were counted from three equivalent locations for neurons and IBA-1 merged VP1 positive cells from six equivalent locations for microglia along the rostrocaudal axis. The cells were marked with the suggested color. Microglia were counted using the MetaMorph neurite outgrowth module (Molecular Devices). The density was obtained by dividing the counted value by the area of each anatomical structure. The anatomical structure was divided into cerebral cortex, cerebral nuclei, fimbria, internal capsule, thalamus, hypothalamus, and midbrain. In the olfactory region, the cerebral cortex was divided into isocortex and olfactory areas, and the hippocampus was separated from the cerebral cortex in the section including the hippocampus. In the case of cerebral nuclei, the striatum and pallidum were largely divided, and the striatum was divided again into the dorsal region, lateral septa complex, and ventral region.

Statistical analysis

All values of experimental data are expressed as mean ± SD. Statistical significance was evaluated using the unpaired t-test, one-way ANOVA, or two-way ANOVA using Graphpad Prism software (Graphpad, La Jolla, CA). Linear regression was used to analyze the correlation between mCherry and EGFP signal using Graphpad Prism software.

Results

CVB3 infection regulates α-syn expression in neurons

To explore whether CVB3 affects α-syn, we infected differentiated SH-SY5Y cells (dSH-SY5Y cells) with CVB3 (MOI 0.25) for 24 h. CVB3 VP1 colocalized with α-syn and the intensity of α-syn in infected cells was increased. Interestingly, we observed that CVB3 infection induced large aggregates of α-syn that completely filled the cytoplasm and pushed the nucleus aside, creating a half-moon appearance. This appearance was clearer in dSH-SY5Y cells overexpressing α-syn (Fig. 1a). In primary cortical neurons, a similar colocalization of VP1 with α-syn observed (Fig. 1b). In contrast, the mRNA level of α-syn was decreased in dSH-SY5Y cells and primary cortical neurons infected with CVB3 (Fig. 1c). Analysis of an

open source database (GSE 19496) also showed that the mRNA level of α-syn in CVB3-infected mouse heart was also decreased compared with that in the control (Supplementary Fig. 1a). Western blot analysis showed that endogenous α-syn was decreased. Interestingly, ectopically overexpressed α-syn was also decreased. It was likely to be more severe as the virus titer increased (Fig. 1d). When we intraperitoneally infected WT mice with CVB3, decreased levels of α-syn mRNA and protein in the brain were also observed (Fig. 1e-f). Given that CVB3 did not infect all cells, these results led us to speculate that α-syn may be regulated differently in both CVB3 infected cells and neighboring cells. To explore this, we compared α-syn levels in both non-infected and infected conditions. Increased α-syn level was observed in CVB3-infected cells and the α-syn level was obviously decreased in neighboring cells near CVB3-infected cells (Fig. 1g). Similar findings were observed in primary cortical neurons (Fig. 1h), suggesting that α-syn was regulated differently in both CVB3-infected cells and neighboring cells. When cells were treated with poly IC, an artificial analog to mimic RNA viral infection [26], α-syn was increased at both the mRNA and protein levels, whereas α-syn aggregates were not observed (Fig. 1i-k). These findings suggested that the observations were CVB3 specific. Analysis of another open source database (GSE 7621) also revealed the decreased mRNA level of α-syn in the brains of patients with PD compared with controls (Supplementary Fig. 1b). These results suggested that CVB3 infection induced large cytosolic aggregates that colocalized with α-syn, and that α-syn expression was differentially regulated between infected cells and neighboring cells.

CVB3 infection induces LB-like inclusion body formation in neurons

CVB3 forms very large autophagy-related structures termed megaphagosomes in murine pancreatic acinar cells as replication complexes [27]. To investigate these large aggregates colocalized with α-syn in more detail, we stained with microtubule-associated protein 1A/1B light chain 3B (LC3), a marker for autophagosomes [28]. These structures completely colocalized with LC3 in dSH-SY5Y cells, α-syn overexpressing (OE) dSH-SY5Y cells and primary cortical neurons (Fig. 2a). These structures also co-stained with pSer129 α-syn antibody in α-syn OE dSH-SY5Y cells and primary cortical neurons (Fig. 2b). The colocalization with ubiquitin, another marker for LB [29], was more clearly observed in α-syn OE dSH-SY5Y cells, suggesting that these structures may be LB-like inclusions (Fig. 2c). Next, we examined these structures by TEM. In the absence of CVB3 infection, intracellular organelles spread throughout the cytoplasm in both dSH-SY5Y cells and α-syn OE dSH-SY5Y cells, whereas the organelles of virus-infected cells were gathered in spherical structures (Fig. 2d). These spherical structures contained various disorganized organelles, consisting large amounts of vesicles, damaged mitochondria, and autophagic components (Fig. 2d), similar to previously observed megaphagosomes [27]. These structures were also similar to previously observed LBs [30]. In addition, replication particles of CVB3 were observed and were more numerous in α-syn OE dSH-SY5Y cells than in dSH-SY5Y cells (Fig. 2e). They were also observed in mouse primary neurons (Fig. 2f). Fibrillar structures were observed in CVB3-infected cells. The width and length of these fibrillar structures in dSH-SY5Y cells were approximately 20 nm and 400 nm, respectively (Fig. 2g). The fibrils were more numerous and longer in α-syn OE dSH-SY5Y cells than in dSH-SY5Y cells

(Fig. 2g). These patterns were also observed in primary cortical neurons from WT and α-syn TG mice (Fig. 2h). These results suggested that CVB3 infection induced LB-like inclusions in neurons. In addition, damaged mitochondria were analyzed as described previously [24]. In the resting condition, there were no differences in mitochondrial morphology between dSH-SY5Y cells and α-syn OE dSH-SY5Y cells. However, after infection with CVB3, damaged mitochondria were increased in dSH-SY5Y cells and even more numerous in α-syn OE dSH-SY5Y cells (Fig. 2i-j), suggesting that mitochondrial damage by CVB3 infection was accelerated by α-syn overexpression.

α-Syn regulates maturation of LB-like inclusion bodies induced by CVB3

We analyzed the relationship between the LB-like inclusion body formed by CVB3 and α-syn in more detail. CVB3 induced different types of LB-like inclusion bodies over time when evaluated by LC3 staining patterns. We classified them into four stages based on the staining pattern of LC3 (Fig. 3a). VP1 protein of CVB3 VP1 was observed, but the state where intracellular LC3 morphology does not differ from uninfected cells was defined as stage 1 (Fig. 3a1). The stage in which the intracellular arrangement of LC3 began to show slight changes was defined as stage 2 (Fig. 3a2), and LC3 began to form a sphere was defined as stage 3 (Fig. 3a3). Finally, the stage in which LC3 formed a complete sphere with strong intensity was defined as stage 4 (Fig. 3a4). It also colocalized with pSer129 α-syn. Over time, the number of inclusion body in stage 4 was increased (Fig. 3b,c), suggesting the maturation of LB-like inclusion body. Interestingly, the number of inclusion bodies in stage 4 was higher in α-syn OE SH-SY5Y cells than in the control (Fig. 3b,c). In addition, in α-syn OE SH-SY5Y cells, LC3 was colocalized to inclusion bodies with higher intensity than control (Fig. 3d,e). Inclusion bodies were more condensed and the proportion of CVB3 present in the inclusion body was also increased (Fig. 3d,e), suggesting that α-syn overexpression accelerated the maturation of inclusion bodies induced by CVB3.

α-Syn regulates replication of CVB3 in neurons

Large autophagosomes induced by CVB3 are replication complexes [31]. Given that α-syn overexpression accelerated the maturation of inclusion bodies induced by CVB3 and that α-syn OE dSH-SY5Y cells displayed greater VP1 intensity in inclusion bodies than in dSH-SY5Y cells, we investigated whether α-syn affected the replication of CVB3. CVB3 replication was increased in α-syn OE SH-SY5Y cells and primary neurons from α-syn TG mice (Fig. 4a), consistent with the TEM analysis (Fig. 2e). Infection with the CVB3 variant co-expressing EGFP (CVB3-EGFP) produced increases in the number of EGFP-positive cells and intensity of EGFP in α-syn OE SH-SY5Y cells (Fig. 4c-e). Additionally, when CVB3-EGFP was used to infect SH-SY5Y cells overexpressing mCherry only or α-syn-mCherry, the intensity of EGFP was positively proportional to that of mCherry in α-syn-mCherry OE SH-SY5Y cells, but not in mCherry only OE SH-SY5Y cells (Fig. 4f,g). The cytotoxicity of CVB3 infection was more severe in α-syn OE SH-SY5Y cells (Fig. 4h), suggesting that α-syn promotes CVB3 replication and related cytotoxicity.

CVB3 and α-syn differentially regulate autophagic activity

CVB3 inhibits the fusion of autophagosomes and lysosomes and uses autophagosomes as replication complexes [31]. To confirm this, we monitored autophagic activity [32, 33]. LC3II levels were increased by CVB3 infection. However, it was not further increased by treatment with bafilomycin A1 (BafA1) (Fig. 5a), suggesting that CVB3 inhibited the late stage of the autophagic process. This was further supported by a significant reduction of lysosomes evaluated by LysoTracker in CVB3-infected dSH-SY5Y cells (Fig. 5b). On the other hand, LC3II levels were increased and treatment with BafA1 further increased LC3II levels in α-syn OE dSH-SY5Y cells (Fig. 5c). p62 levels were decreased (Fig. 5d), suggesting that α-syn overexpression increased autophagic flux, which agreed with a previous study [34]. We further analyzed open source database information. Overexpression of human α-syn using a lentiviral vector in mouse midbrain neurons revealed that the cluster of transcriptome was characterized by a "positive regulation of macroautophagy" (GO:0016239) in gene ontology (GO) analysis compared to control (GSE70368) (Supplementary Fig. 3a,b). In addition, "autophagosome maturation" (GO:0097352) in the induced pluripotent stem cells (iPSC) of α-syn (SNCA) triplicated family (GSE30792) and "lysosome organization" (GO:0007040) in the mouse striatum tissue of human α-syn TG mice (GSE116010) were also higher than in controls (Supplementary Fig. 3a,b). These findings supported our data. Compared with the control, CVB3 infection further increased LC3 II levels, and the treatment with BafA1 induced similar results in α-syn OE dSH-SY5Y cells (Fig. 5e,f). These results suggested that α-syn overexpression promoted autophagic flux and accelerated the formation of autophagosomes, which provided more replication centers for CVB3.

α-Syn regulates CVB3 replication in mouse brains

To confirm whether CVB3 also interacts with α-syn in the brain, CVB3 was intraperitoneally injected into mice. At day 7 postinfection (PI), the detection of CVB3 was more pronounced in brains from α-syn TG mice, compared with WT mice (Fig. 6a). The *in vivo* data were consistent with the *in vitro* data. IHC analysis of the brain from WT mice detected CVB3 in the olfactory area, anterior cingulate area, lateral septal nucleus, hippocampal region, fimbria, corticospinal tract, and hypothalamus, mainly along the ventricles, which were colocalized with the IBA-1 microglial marker. In addition, CVB3 was also detected in the hippocampus, lateral thalamus, and midbrain, which colocalized with the TUJ-1 neuronal marker. CVB3 did not colocalize with the GFAP astrocyte marker (Fig. 6b,c), suggesting that CVB3 was detected in the brain and infected with microglia and neurons, but not astrocytes.

CVB3 was observed in neurons located in the hippocampus, lateral thalamus, and midbrain at day 4 PI. At day 7 PI, the number of neurons infected with CVB3 was increased compared to that in the mice at day 4 PI (Fig. 6d). At day 28 PI, the number of midbrain neurons infected with CVB3 was clearly increased whereas the number of neurons located in other regions infected by CVB3 was relatively decreased (Fig. 6d). The pattern of infected neurons was more accelerated in α-syn TG mice than in WT mice. At day 4 PI, the number of neurons infected with CVB3 was not significantly different between WT mice and α-syn TG mice, but relatively more neurons infected with CVB3 were observed in the hippocampus of α-syn

TG mice, compared with that of WT mice (Fig. 6d). At day 7 PI, the pattern of infected neurons in TG mice was comparable with that in WT mice at day 28 PI (Fig. 6d). The number of CVB3 infected microglia increased at day 7 PI (Fig. 6e). At day 28 PI, the number of CVB3 infected microglia was similar to that at day 7 PI (Fig. 6e). The number of CVB3 infected microglia was also higher in TG mice than in WT mice during the same period (Fig. 6e).

At day 28 PI, the cleaved caspase 3 marker for apoptosis, was focally observed throughout the brain of WT mice (Fig. 6f and Supplementary Fig. 3). This observation was also evident in TG mice at day 7 PI, which was comparable to that in WT mice at day 28 PI (Fig. 6g). Additionally, CVB3 were infected dopaminergic neurons located in the substantia nigra (Fig. 6h). The numbers of tyrosine hydroxylase (TH)-positive cells were decreased in the substantia nigra from CVB3 infected mice at day 28 PI, compared with the control, which was also comparable to that in TG mice at day 7 PI (Fig. 6i,j).

We then monitored the survival rate of both WT and α-syn TG mice. The survival of α-syn TG mice was poorer than survival of WT mice. Weight loss was more severe in α-syn TG mice. The findings suggested that α-syn TG mice were more susceptible to CVB3 infection (Fig. 6k). CVB3 is a cardiotropic virus that induces myocarditis [16]. Therefore, we monitored myocardial damage and replication of CVB3 in the heart. Heart damage and the level of VP1 in the myocardium from both mice groups were similar (Supplementary Fig. 4a,b). The findings suggested that the difference in the survival rate of both mice groups may not have been due to cardiac damage. These results suggested that CVB3 infection in the mouse brain caused neuronal death, including dopaminergic neurons located in the substantia nigra, and that α-syn accelerated the replication of CVB3 and neuronal death by CVB3.

CVB3 induces α-syn inclusions in mouse brains

Next, we examined the colocalization of α-syn and CVB3 VP1 in the brain of mice infected with CVB3. We did not observe colocalization of α-syn and CVB3 VP1 in the brains of WT or α-syn TG mice. Instead, at day 7 PI, a few α-syn inclusions in the cell body were observed in the interpeduncular nucleus from WT mice where CVB3 was infected and the intensity of α-syn was lower than that of the control (Fig. 7a). However, α-syn inclusions were not stained with the pSer129 α-syn antibody. In α-syn TG mice, more α-syn inclusions were observed in the same region, although they were also not stained with the pSer129 α-syn antibody (Fig. 7a). We performed western blotting to detect pSer129 α-syn. At day 28 PI in WT mice, pSer 129 α-syn was weakly detected and a decrease in α-syn expression was observed (Fig. 7b). Similar observations were made in α-syn TG mice at day 7 PI, suggesting that α-syn inclusions were induced by CVB3 infection and were accelerated by α-syn overexpression (Fig. 7c).

Discussion

Despite much research, the pathogenesis of PD remains elusive. Both genetic and environmental factors in combination are suspected to contribute to the pathogenesis of PD [35]. LBs are the main pathological hallmark of PD. Additionally, Lewy pathology progressively involves more regions of the nervous system as the disease advances, and it is present prior to the appearance of motor symptoms in PD [8],

Accordingly, it is important to identify which factors initiate Lewy pathology to understand the pathogenesis of PD. Several factors are suspected to be triggers of Lewy pathology. Several environmental factors that contribute include pathogens, such as influenza virus, environmental pollutants like pesticides, heavy metals, and head trauma [36]. In particular, viral infection has long been considered a risk factor for neurodegenerative diseases [13]. The present data demonstrate that CVB3 interacts with α-syn to promote PD.

Concerning the influence of CVB3 on α-syn, CVB3 infection induces very large autophagy-related structures ranging 10–20 μm in diameter in neurons. These structures colocalize with LC3 and have a similar morphology to that of megaphagosomes shown in pancreatic acinar cells [27]. They also stain with α-syn, pSer129 α-syn, and ubiquitin antibodies, suggesting a resemblance to LBs. LBs have significant morphological diversity and are heterogeneous in their shape, biochemical composition, and organization [29]. Examinations of the brains of patients with PD using super-high resolution microscopy based on stimulated emission depletion (STED) revealed LBS with crowded organelles and lipid membranes. This prompted the proposal that α-syn may modulate the compartmentalization and function of membranes and organelles in LB-affected cells [30]. A recent report demonstrated the formation of filament-like structures accompanying the sequestration of lipids, organelles, and endomembrane structures using a seeding-based model of α-syn fibrillization, which recapitulated the features of LBs observed in the brains of patients with PD [37]. Likewise, our TEM findings also suggested that CVB3 infection resulted in the clustering of several organelles in the perinuclear space in neurons. The crowded organelles contained damaged mitochondria and many fibrillar structures surrounded the organelles. The number of fibrillar structures in α-syn OE dSH-SY5Y cells was higher than that in dSH-SY5Y cells. These structures in α-syn OE dSH-SY5Y cells were also longer than those in dSH-SY5Y cells. Given that α-syn fibrils exhibit 20 nm diameter *in vitro* [38], these observations suggested that these fibrillar structures may be α-syn fibrils. Additionally, the process of LB formation consists of several stages [39, 40]. CVB3 induced different types of LB-like inclusion bodies over time, which may reflect the maturation of the inclusion bodies. In α-syn OE cells, the maturation of these inclusions was accelerated and inclusion bodies were more condensed, suggesting that α-syn may regulate the maturation of inclusion bodies as a major component. In addition, mitochondrial damage was induced by CVB3, which was more in α-syn OE dSH-SY5Y cells. The observations are supported in part by previous studies demonstrating that α-syn localizes in mitochondria and α-syn OE cells exhibit mitochondrial dysfunction [41–43]. We demonstrated that CVB3 inhibited the late stage of the autophagic process in dSH-SY5Y cells, consistent with a previous study [27]. It is well known that α-syn is somewhat degraded through autophagy in cells [44–46], although other mechanisms have also been reported to be involved in α-syn degradation [47]. Blocked late stage autophagy has been reported to cause α-syn accumulation [48]. Accordingly, the use of autophagy machinery by CVB3 may induce the formation of LB-like inclusions associated with α-syn.

Although CVB3 induced large inclusion bodies containing α-syn, its expression was decreased. We confirmed this using *in vitro* and *in vivo* model systems, and open source data from CVB3-infected hearts of mice. In particular, neighboring cells may be more affected. How α-syn expression is regulated

differentially requires further investigation. A previous report demonstrated that WNV induced α-syn expression, and α-syn was proposed as a viral restriction factor [21]. We also observed that treatment with polyIC increased α-syn expression in dSH-SY5Y cells, suggesting that α-syn expression can be regulated by viral infection. However, the decrease in α-syn expression may be CVB3 specific. Interestingly, decreased α-syn mRNA in brains of patients with PD has been described [49, 50]. These findings are contentious due to several technical issues, including sampling and normalization methods. Our analysis of open data sources from patients with PD also confirmed it. Therefore, CVB3 infection may reflect patients with PD.

When we infected mice with CVB3, CVB3 infection first appeared in the region of several anatomical structures along the ventricles, suggesting the route of CVB3 into the CNS from the periphery. Neuron and microglia infection progressed with time to other regions. In neurons, CVB3 was observed in the hippocampus, lateral thalamus, and midbrain in the brain of mice at day 4 PI. Although we observed the colocalization of CVB3 with α-syn *in vitro*, we could not observe the colocalization in the brain of mice infected with CVB3. Instead, we observed α-syn aggregation in the cell bodies of neurons located in the midbrain of WT mice at day 28 PI, and more neurons containing cytosolic α-syn aggregation were observed in α-syn TG mice at day 7 PI. In addition, western blot analysis indicated that pSer129 α-syn was slightly increased in the brain infected with CVB3. In a previous report [36], the authors proposed that triggers alone are usually insufficient for PD to develop. Triggers often act transiently, with the triggering event lasting a few weeks or months and occurring relatively early in the life of individuals that develop PD. Accordingly, CVB3 infection may act transiently. It alone may not induce LB formation in the brain, unlike *in vitro*. Alternatively, the neuronal α-syn aggregation observed in our *in vivo* system may not reach the same mature stage as the PD LB, because our *in vivo* model system is not adequate for prolonged observations due to the high mortality of CVB3 infection in C57BL/6 mice [51]. The long-term consequences of CVB3 infection in the CNS are largely unknown. However, these viruses persist, and the presence of viral RNA by itself is potentially pathogenic in some cases including schizophrenia [52] and amyotrophic lateral sclerosis [53]. Interestingly, CVB3 infected BALB/c mice, which are more susceptible to chronic CVB3 infection, reportedly showed TDP-43 aggregation in the hippocampal region at 90 days PI [54]. In addition, it has been reported that cytosolic aggregates as well as soluble oligomers, which were not observed in healthy controls, were observed in the heart of patients with dilated cardiomyopathy, which is suspected to be caused by CVB3 infections [55, 56]. Congo red merged islet amyloid polypeptide was also seen in pancreatic biopsies of patients with type 1 diabetes, suggesting that these aggregations may be caused by enteroviruses stressing beta cells [57]. Accordingly, viral-induced intracellular protein inclusions do not restrict neurons; rather, they are a general phenomenon.

In this study, we observed that α-syn expression regulated CVB3 replication. Overexpression of α-syn increased CVB3 replication and CVB3 induced cytotoxicity. We confirmed this *in vivo* in brains of α-syn TG mice. CVB3 replication was increased and the spread of CVB3 infected regions was also accelerated in α-syn TG mice compared with control mice. In addition, CVB3 infection induced neuronal cell death, especially dopaminergic neuronal cell death in the substantia nigra. Interestingly and supporting our observation, patients with chronic EV71 encephalitis whose symptoms persisted for more than 2 months

displayed damage in most of the midbrain, including the substantia nigra [58]. Dopaminergic neuronal cell death in the substantia nigra was also accelerated in α-syn TG mice. Furthermore, α-syn TG mice survived less than WT mice. A previous report demonstrated that α-syn expression inhibits WNV growth and replication, resulting in increased mortality of α-syn knock-out mice [21], which contradicts our findings, demonstrating that α-syn TG mice show more CVB3 replication and a lower survival rate after CVB3 infection. We cannot completely explain the discrepancy between these results. The balance of the amount of α-syn in the brain may be important for the regulation of viral infection. Nevertheless, this could be explained by the viral usage of autophagy. Previous studies have suggested that CVB3 uses autophagosomes as their replication centers by inhibiting the binding of autophagosomes to lysosomes [27, 59, 60]. The induction of autophagy in neurons was also associated with increased CVB3 replication [59–61]. Given that an increase in α-syn expression accelerated autophagic flux, this environment favors the replication of CVB3. In contrast, autophagy is known to inhibit WNV replication [62, 63]. Accordingly, it may be virus-specific, and autophagy in both viruses may explain this discrepancy.

The epidemiologic links suggest that viral exposure over time may increase the risk for PD, although it is unclear whether any specific viral infection causes PD. It could be related to direct virus-induced cytotoxicity or virus-related inflammation [64–66]. Influenza viral infections induce parkinsonian symptoms and a significant increase in phosphorylation and aggregation of α-syn [67, 68]. Repeated viral infection may induce α-syn expression or/and α-syn aggregation, and chronic viral infection also induces further inflammation, which may initiate and progress PD. Likewise, we observed that α-syn responded to CVB3 infection. CVB3 infection regulated α-syn expression and aggregation. α-Syn may function as a defense mechanism of the host cells against viral infection. The finding that infecting CVB3 interacted with α-syn in various ways suggests an unexpected role of α-syn in the pathogenesis of PD. Further studies are needed to explore this in more detail.

Conclusions

We investigated the relationship between CVB3 infection and α-syn. CVB3 infection induced α-syn associated inclusion body formation in neurons as a trigger. These inclusion bodies contained clustered organelles including damaged mitochondria with α-syn fibrils. α-Syn overexpression accelerated inclusion body formation and induced more concentric inclusion bodies. Brains from CVB3 infected mice harbored α-syn aggregates in the cell body of the midbrain. The data indicate that CVB3 infection blocks the late stage of autophagy, inducing inclusion body formation containing α-syn fibrils. Overexpression of α-syn favors CVB3 replication and related cytotoxicity. The survival of α-syn TG mice was poor. CVB3 replication was more extensive in these mice, with further neuronal cell death, including dopaminergic neurons. α-Syn overexpression accelerated autophagic flux, which favored the replication of CVB3. The collective findings clarify the mechanism of LB formation and the pathogenesis of PD associated with CVB3 infection.

Abbreviations

PD : Parkinson's disease

α-Syn : α-Synuclein

CVB3 : coxsackievirus B3

LBs : Lewy bodies

AD : Alzheimer’s disease

WNV : West Nile virus

LC3 : microtubule-associated protein 1A/1B light chain 3B

GFAP : glial fibrillary acidic protein

GAPDH : glyceraldehyde 3-phosphate dehydrogenase

RA : retinoic acid

Baf A1 : bafilomycin A1

poly IC : polyinosine:polycytidylic acid

EBD : Evans blue dye

TG : transgenic

NSE : neuron specific enolase

WT : wild-type

KO : knockout

DMEM : Dulbecco’s modified Eagle’s medium

FBS : fetal bovine serum

MOI : multiplicity of infection

IP injection : intraperitoneal injection

PFU : plaque forming units

PBS : phosphate-buffered saline

RT-PCR : reverse transcription polymerase chain reaction

ICC : immunocytochemistry

BSA : bovine serum albumin

ECL : enhanced chemiluminescence system

h : human

m : mouse

SNCA : α-Synuclein

TEM : transmission electron microscopy

LDH : lactate dehydrogenase

IHC : immunocytochemistry

PBST : PBS containing 0.2% Triton X-100

GO : gene ontology

DAPI : 4',6-diamidino-2-phenylindole

CVB3-EGFP : CVB3 variant co-expressing EGFP

DEG : differential expressed genes

GEO : gene expression omnibus

iPSC : induced pluripotent stem cells

PI : postinfection

CTX : cortex

MOB : main olfactory bulb

AON : anterior olfactory nucleus

LSX : lateral septal complex

HY : hypothalamus

ACA : anterior cingulate area

fxs : fornix system

MO : somatomotor area

HCF : Hippocampal formation

TH : thalamus

CP : caudoputamen

Cst : corticospinal tract

RSP : retrosplenial area

PRT : pretectal region

MRN : midbrain reticular nucleus

SN : substantia nigra

c-caspase3 : cleaved caspase3

Hp - hippocampus

TH : tyrosine hydroxylase

DAB : diaminobenzidine

SNc : substantia nigra pars compacta

STED : stimulated emission depletion

MAVS : mitochondrial antiviral signaling protein

EV71 : enterovirus71

Declarations

Ethics approval and consent to participate

All animal procedures were conducted according to the guidelines established by the Ajou University School of Medicine Ethics Review Committee (IACUC No. 2016-0047).

Consent for publication

Not applicable

Availability of data and materials

The datasets used and/or analysed during the current study are available from the corresponding author on reasonable request.

Competing interests

The authors declare that they have no competing interests

Funding

This research was supported by the National Research Foundation of Korea (NRF) grants funded by the Korean government (Ministry of Science and ICT) (Grant No. NRF-2017R1E1A1A01073713, NRF-2019R1A5A2026045).

Authors' contributions

SJP, UJ, and SMP designed the study. SJP and UJ performed the experiments. SJP, UJ, and SMP analyzed and discussed the data. SJP and SMP wrote and edited the manuscript. All authors read and approved the final manuscript.

Acknowledgements

We thank to Dr. E. Jeon (Samsung Medical Center, Seoul, Korea) for kindly providing the H3 variant of CVB3, the Woodruff strain, and EGFP-CVB3. We also thank NIFDS for providing C56BL/6-Tg (NSE-haSyn)Korl mice and their information.

References

1. Poewe W, Seppi K, Tanner CM, Halliday GM, Brundin P, Volkmann J, Schrag A-E, Lang AE: **Parkinson disease.** *Nature reviews Disease primers* 2017, **3:**17013.
2. Kalia LV, Lang AE: **Parkinson's disease.** *Lancet* 2015, **386:**896-912.
3. Spillantini MG, Schmidt ML, Lee VM, Trojanowski JQ, Jakes R, Goedert M: **Alpha-synuclein in Lewy bodies.** *Nature* 1997, **388:**839-840.
4. Eschbach J, Danzer KM: **α-Synuclein in Parkinson's disease: pathogenic function and translation into animal models.** *Neurodegenerative Diseases* 2014, **14:**1-17.
5. Mullin S, Schapira A: **The genetics of Parkinson's disease.** *British medical bulletin* 2015, **114:**39-52.

6. Nalls MA, Pankratz N, Lill CM, Do CB, Hernandez DG, Saad M, DeStefano AL, Kara E, Bras J, Sharma M: **Large-scale meta-analysis of genome-wide association data identifies six new risk loci for Parkinson's disease.** *Nature genetics* 2014, **46:**989.
7. Satake W, Nakabayashi Y, Mizuta I, Hirota Y, Ito C, Kubo M, Kawaguchi T, Tsunoda T, Watanabe M, Takeda A: **Genome-wide association study identifies common variants at four loci as genetic risk factors for Parkinson's disease.** *Nature genetics* 2009, **41:**1303.
8. Braak H, Del Tredici K, Rub U, de Vos RA, Jansen Steur EN, Braak E: **Staging of brain pathology related to sporadic Parkinson's disease.** *Neurobiology of aging* 2003, **24:**197-211.
9. Braak H, Del Tredici K: **Invited Article: Nervous system pathology in sporadic Parkinson disease.** *Neurology* 2008, **70:**1916-1925.
10. Volpicelli-Daley L, Brundin P: **Prion-like propagation of pathology in Parkinson disease.** *Handb Clin Neurol* 2018, **153:**321-335.
11. Vargas JY, Grudina C, Zurzolo C: **The prion-like spreading of alpha-synuclein: From in vitro to in vivo models of Parkinson's disease.** *Ageing Res Rev* 2019, **50:**89-101.
12. Tofaris GK, Goedert M, Spillantini MG: **The Transcellular Propagation and Intracellular Trafficking of alpha-Synuclein.** *Cold Spring Harb Perspect Med* 2017, **7**.
13. Jang H, Boltz DA, Webster RG, Smeyne RJ: **Viral parkinsonism.** *Biochimica et Biophysica Acta (BBA)-Molecular Basis of Disease* 2009, **1792:**714-721.
14. Tulisiak CT, Mercado G, Peelaerts W, Brundin L, Brundin P: **Can infections trigger alpha-synucleinopathies?** *Prog Mol Biol Transl Sci* 2019, **168:**299-322.
15. Garmaroudi FS, Marchant D, Hendry R, Luo H, Yang D, Ye X, Shi J, McManus BM: **Coxsackievirus B3 replication and pathogenesis.** *Future microbiology* 2015, **10:**629-653.
16. Tam PE: **Coxsackievirus myocarditis: interplay between virus and host in the pathogenesis of heart disease.** *Viral immunology* 2006, **19:**133-146.
17. Muir P, Van Loon A: **Enterovirus infections of the central nervous system.** *Intervirology* 1997, **40:**153-166.
18. Chapman NM, Kim KS: **Persistent coxsackievirus infection: enterovirus persistence in chronic myocarditis and dilated cardiomyopathy.** *Curr Top Microbiol Immunol* 2008, **323:**275-292.
19. Alidjinou EK, Sané F, Engelmann I, Geenen V, Hober D: **Enterovirus persistence as a mechanism in the pathogenesis of type 1 diabetes.** *Discov Med* 2014, **18:**273-282.
20. Dourmashkin RR, McCall SA, Dourmashkin N, Hannah MJ: **Virus-like particles and enterovirus antigen found in the brainstem neurons of Parkinson's disease.** *F1000Research* 2018, **7**.
21. Beatman EL, Massey A, Shives KD, Burrack KS, Chamanian M, Morrison TE, Beckham JD: **Alpha-synuclein expression restricts RNA viral infections in the brain.** *Journal of virology* 2016, **90:**2767-2782.
22. Choi YR, Cha SH, Kang SJ, Kim JB, Jou I, Park SM: **Prion-like Propagation of alpha-Synuclein Is Regulated by the FcgammaRIIB-SHP-1/2 Signaling Pathway in Neurons.** *Cell Rep* 2018, **22:**136-148.

23. Yoon S, Park S, Han J, Kang J, Kim J, Lee J, Park S, Shin H, Kim K, Yun M: **Caspase-dependent cell death-associated release of nucleosome and damage-associated molecular patterns.** *Cell death & disease* 2014, **5:**e1494-e1494.
24. Shults NV, Kanovka SS, Ten Eyck JE, Rybka V, Suzuki YJ: **Ultrastructural changes of the right ventricular myocytes in pulmonary arterial hypertension.** *Journal of the American Heart Association* 2019, **8:**e011227.
25. Robinson SM, Tsueng G, Sin J, Mangale V, Rahawi S, McIntyre LL, Williams W, Kha N, Cruz C, Hancock BM: **Coxsackievirus B exits the host cell in shed microvesicles displaying autophagosomal markers.** *PLoS pathogens* 2014, **10:**e1004045.
26. Alexopoulou L, Holt AC, Medzhitov R, Flavell RA: **Recognition of double-stranded RNA and activation of NF-κB by Toll-like receptor 3.** *Nature* 2001, **413:**732.
27. Kemball CC, Alirezaei M, Flynn CT, Wood MR, Harkins S, Kiosses WB, Whitton JL: **Coxsackievirus infection induces autophagy-like vesicles and megaphagosomes in pancreatic acinar cells in vivo.** *Journal of virology* 2010, **84:**12110-12124.
28. Shibutani ST, Saitoh T, Nowag H, Münz C, Yoshimori T: **Autophagy and autophagy-related proteins in the immune system.** *Nature immunology* 2015, **16:**1014-1024.
29. Wakabayashi K, Tanji K, Odagiri S, Miki Y, Mori F, Takahashi H: **The Lewy body in Parkinson's disease and related neurodegenerative disorders.** *Molecular neurobiology* 2013, **47:**495-508.
30. Shahmoradian SH, Lewis AJ, Genoud C, Hench J, Moors TE, Navarro PP, Castaño-Díez D, Schweighauser G, Graff-Meyer A, Goldie KN: **Lewy pathology in Parkinson's disease consists of crowded organelles and lipid membranes.** *Nature Neuroscience* 2019, **22:**1099.
31. Wong J, Zhang J, Si X, Gao G, Mao I, McManus BM, Luo H: **Autophagosome supports coxsackievirus B3 replication in host cells.** *Journal of virology* 2008, **82:**9143-9153.
32. Klionsky DJ, Abdelmohsen K, Abe A, Abedin MJ, Abeliovich H, Acevedo Arozena A, Adachi H, Adams CM, Adams PD, Adeli K, et al: **Guidelines for the use and interpretation of assays for monitoring autophagy (3rd edition).** *Autophagy* 2016, **12:**1-222.
33. Yoshii SR, Mizushima N: **Monitoring and Measuring Autophagy.** *Int J Mol Sci* 2017, **18:**1865.
34. Xilouri M, Vogiatzi T, Vekrellis K, Park D, Stefanis L: **Abberant α-synuclein confers toxicity to neurons in part through inhibition of chaperone-mediated autophagy.** *PloS one* 2009, **4:**e5515.
35. Klein C, Schlossmacher MG: **Parkinson disease, 10 years after its genetic revolution: multiple clues to a complex disorder.** *Neurology* 2007, **69:**2093-2104.
36. Johnson ME, Stecher B, Labrie V, Brundin L, Brundin P: **Triggers, Facilitators, and Aggravators: Redefining Parkinson's Disease Pathogenesis.** *Trends Neurosci* 2019, **42:**4-13.
37. Mahul-Mellier AL, Burtscher J, Maharjan N, Weerens L, Croisier M, Kuttler F, Leleu M, Knott GW, Lashuel HA: **The process of Lewy body formation, rather than simply alpha-synuclein fibrillization, is one of the major drivers of neurodegeneration.** *Proc Natl Acad Sci U S A* 2020, **117:**4971-4982.

38. Lashuel HA: **Do Lewy bodies contain alpha-synuclein fibrils? and Does it matter? A brief history and critical analysis of recent reports.** *Neurobiology of disease* 2020**:**104876.

39. Wakabayashi K, Hayashi S, Kakita A, Yamada M, Toyoshima Y, Yoshimoto M, Takahashi H: **Accumulation of alpha-synuclein/NACP is a cytopathological feature common to Lewy body disease and multiple system atrophy.** *Acta Neuropathol* 1998, **96:**445-452.

40. Katsuse O, Iseki E, Marui W, Kosaka K: **Developmental stages of cortical Lewy bodies and their relation to axonal transport blockage in brains of patients with dementia with Lewy bodies.** *J Neurol Sci* 2003, **211:**29-35.

41. Devi L, Raghavendran V, Prabhu BM, Avadhani NG, Anandatheerthavarada HK: **Mitochondrial import and accumulation of alpha-synuclein impair complex I in human dopaminergic neuronal cultures and Parkinson disease brain.** *J Biol Chem* 2008, **283:**9089-9100.

42. Nakamura K, Nemani VM, Azarbal F, Skibinski G, Levy JM, Egami K, Munishkina L, Zhang J, Gardner B, Wakabayashi J, et al: **Direct membrane association drives mitochondrial fission by the Parkinson disease-associated protein alpha-synuclein.** *J Biol Chem* 2011, **286:**20710-20726.

43. Park JH, Burgess JD, Faroqi AH, DeMeo NN, Fiesel FC, Springer W, Delenclos M, McLean PJ: **Alpha-synuclein-induced mitochondrial dysfunction is mediated via a sirtuin 3-dependent pathway.** *Mol Neurodegener* 2020, **15:**5.

44. Paxinou E, Chen Q, Weisse M, Giasson BI, Norris EH, Rueter SM, Trojanowski JQ, Lee VM, Ischiropoulos H: **Induction of alpha-synuclein aggregation by intracellular nitrative insult.** *The Journal of neuroscience : the official journal of the Society for Neuroscience* 2001, **21:**8053-8061.

45. Vogiatzi T, Xilouri M, Vekrellis K, Stefanis L: **Wild type α-synuclein is degraded by chaperone-mediated autophagy and macroautophagy in neuronal cells.** *Journal of Biological Chemistry* 2008, **283:**23542-23556.

46. Alvarez-Erviti L, Rodriguez-Oroz MC, Cooper JM, Caballero C, Ferrer I, Obeso JA, Schapira AH: **Chaperone-mediated autophagy markers in Parkinson disease brains.** *Archives of neurology* 2010, **67:**1464-1472.

47. Stefanis L, Emmanouilidou E, Pantazopoulou M, Kirik D, Vekrellis K, Tofaris GK: **How is alpha-synuclein cleared from the cell?** *Journal of neurochemistry* 2019, **150:**577-590.

48. Ejlerskov P, Hultberg JG, Wang J, Carlsson R, Ambjorn M, Kuss M, Liu Y, Porcu G, Kolkova K, Friis Rundsten C, et al: **Lack of Neuronal IFN-beta-IFNAR Causes Lewy Body- and Parkinson's Disease-like Dementia.** *Cell* 2015, **163:**324-339.

49. Neystat M, Lynch T, Przedborski S, Kholodilov N, Rzhetskaya M, Burke RE: **Alpha-synuclein expression in substantia nigra and cortex in Parkinson's disease.** *Mov Disord* 1999, **14:**417-422.

50. Kingsbury AE, Daniel SE, Sangha H, Eisen S, Lees AJ, Foster OJ: **Alteration in alpha-synuclein mRNA expression in Parkinson's disease.** *Mov Disord* 2004, **19:**162-170.

51. Blyszczuk P: **Myocarditis in Humans and in Experimental Animal Models.** *Front Cardiovasc Med* 2019, **6:**64.

52. Rantakallio P, Jones P, Moring J, Von Wendt L: **Association between central nervous system infections during childhood and adult onset schizophrenia and other psychoses: a 28-year follow-up.** *International journal of epidemiology* 1997, **26:**837-843.

53. Woodall CJ, Graham DI: **Evidence for neuronal localisation of enteroviral sequences in motor neurone disease/amyotrophic lateral sclerosis by in situ hybridization.** *Eur J Histochem* 2004, **48:**129-134.

54. Xue YC, Ruller CM, Fung G, Mohamud Y, Deng H, Liu H, Zhang J, Feuer R, Luo H: **Enteroviral Infection Leads to Transactive Response DNA-Binding Protein 43 Pathology in Vivo.** *Am J Pathol* 2018, **188:**2853-2862.

55. Kostin S, Pool L, Elsässer A, Hein S, Drexler HC, Arnon E, Hayakawa Y, Zimmermann R, Bauer E, Klövekorn W-P: **Myocytes die by multiple mechanisms in failing human hearts.** *Circulation research* 2003, **92:**715-724.

56. Sanbe A, Osinska H, Saffitz JE, Glabe CG, Kayed R, Maloyan A, Robbins J: **Desmin-related cardiomyopathy in transgenic mice: a cardiac amyloidosis.** *Proceedings of the National Academy of Sciences* 2004, **101:**10132-10136.

57. Westermark GT, Krogvold L, Dahl-Jørgensen K, Ludvigsson J: **Islet amyloid in recent-onset type 1 diabetes—the DiViD study.** *Upsala journal of medical sciences* 2017, **122:**201-203.

58. Shen WC, Chiu HH, Chow KC, Tsai CH: **MR imaging findings of enteroviral encephaloymelitis: an outbreak in Taiwan.** *AJNR Am J Neuroradiol* 1999, **20:**1889-1895.

59. Jackson WT, Giddings Jr TH, Taylor MP, Mulinyawe S, Rabinovitch M, Kopito RR, Kirkegaard K: **Subversion of cellular autophagosomal machinery by RNA viruses.** *PLoS biology* 2005, **3:**e156.

60. Kirkegaard K, Taylor MP, Jackson WT: **Cellular autophagy: surrender, avoidance and subversion by microorganisms.** *Nature Reviews Microbiology* 2004, **2:**301.

61. Yoon SY, Ha YE, Choi JE, Ahn J, Lee H, Kweon HS, Lee JY, Kim DH: **Coxsackievirus B4 uses autophagy for replication after calpain activation in rat primary neurons.** *J Virol* 2008, **82:**11976-11978.

62. Kobayashi S, Orba Y, Yamaguchi H, Takahashi K, Sasaki M, Hasebe R, Kimura T, Sawa H: **Autophagy inhibits viral genome replication and gene expression stages in West Nile virus infection.** *Virus research* 2014, **191:**83-91.

63. Shoji-Kawata S, Sumpter R, Leveno M, Campbell GR, Zou Z, Kinch L, Wilkins AD, Sun Q, Pallauf K, MacDuff D: **Identification of a candidate therapeutic autophagy-inducing peptide.** *Nature* 2013, **494:**201.

64. Jang H, Boltz DA, Webster RG, Smeyne RJ: **Viral parkinsonism.** *Biochim Biophys Acta* 2009, **1792:**714-721.

65. Jang H, Boltz D, McClaren J, Pani AK, Smeyne M, Korff A, Webster R, Smeyne RJ: **Inflammatory effects of highly pathogenic H5N1 influenza virus infection in the CNS of mice.** *Journal of Neuroscience* 2012, **32:**1545-1559.

66. Sadasivan S, Zanin M, O'Brien K, Schultz-Cherry S, Smeyne RJ: **Induction of microglia activation after infection with the non-neurotropic A/CA/04/2009 H1N1 influenza virus.** *PloS one* 2015, **10**.

67. Jang H, Boltz D, Sturm-Ramirez K, Shepherd KR, Jiao Y, Webster R, Smeyne RJ: **Highly pathogenic H5N1 influenza virus can enter the central nervous system and induce neuroinflammation and neurodegeneration.** *Proceedings of the National Academy of Sciences* 2009, **106:**14063-14068.

68. Marreiros R, Müller-Schiffmann A, Trossbach SV, Prikulis I, Hänsch S, Weidtkamp-Peters S, Moreira AR, Sahu S, Soloviev I, Selvarajah S: **Disruption of cellular proteostasis by H1N1 influenza A virus causes α-synuclein aggregation.** *Proceedings of the National Academy of Sciences* 2020, **117:**6741-6751.

Figures

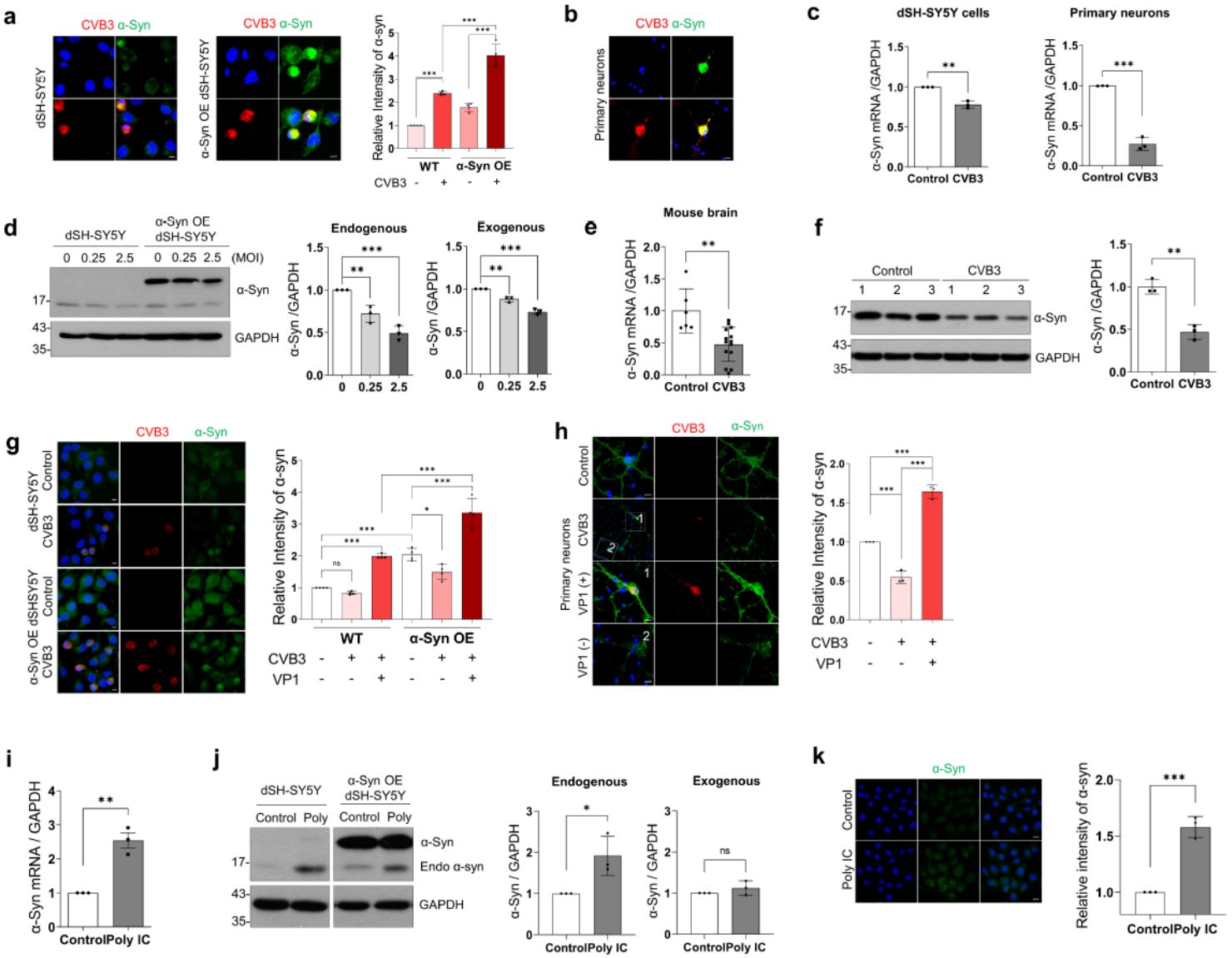

Figure 1

CVB3 infection regulates α-syn expression in neurons. a Immunocytochemistry (ICC) images of WT and α-syn OE dSH-SY5Y cells infected with CVB3. The intensity of α-syn (green) was analyzed (n=4). b ICC images of mouse primary cortical neurons infected with CVB3. Scale bar indicates 10 μm. Blue indicates 4',6-diamidino-2-phenylindole (DAPI). c The relative level of α-syn mRNA expression between control and CVB3 infected cells (n=3). d WT and α-syn OE dSH-SY5Y cells were infected with CVB3 of indicated MOI. Western blot was performed and protein levels were quantified. e The relative level of α-syn mRNA expression between control (n = 6) and CVB3 infected mice brain hemisphere (n = 14) after 4 days intraperitoneal (IP) injection with 1.0 x 106 plaque forming units (PFU) of CVB3. f The relative level of α-syn expression between control (n = 3) and CVB3 infected mice brain hemisphere (n = 3) after 7 days IP injection with 1.0 x 106 PFU of CVB3. Western blot was performed and protein levels were quantified. g-h ICC images of control and CVB3 infected WT, α-syn OE dSH-SY5Y cells (g) and mouse primary cortical neurons (h), which were infected with CVB3. α-Syn (green) intensity of indicated condition was analyzed (n=3 or 4). Scale bar indicates 10 μm. Blue indicates DAPI. i The relative level of α-syn mRNA expression between control and 1 ug/ml poly IC transfected dSH-SY5Y cells for 4 h (n=3). j WT and α-syn OE dSH-SY5Y cells transfected with 1 ug/ml poly IC for 24 h. Western blot was performed and protein levels were quantified. k ICC image of control and 1 ug/ml polyIC transfected dSH-SY5Y cells for 24 h. The intensity of α-syn (green) was analyzed (n=3). Scale bar indicates 20 μm. Blue indicates DAPI. dSH-SY5Y cells and primary cortical neuron were infected with CVB3 of 0.25 and 5 MOI, respectively, for 24 hours. *$p < 0.05$, **$p < 0.01$, or ***$p < 0.001$ versus indicated groups. One-way ANOVA (a, d, g, h) with Tukey's post hoc test; unpaired t-test (c, e, f, i-k). All images are representative of three or more independent experiments. All intensity values were also derived from three or more independent experiments.

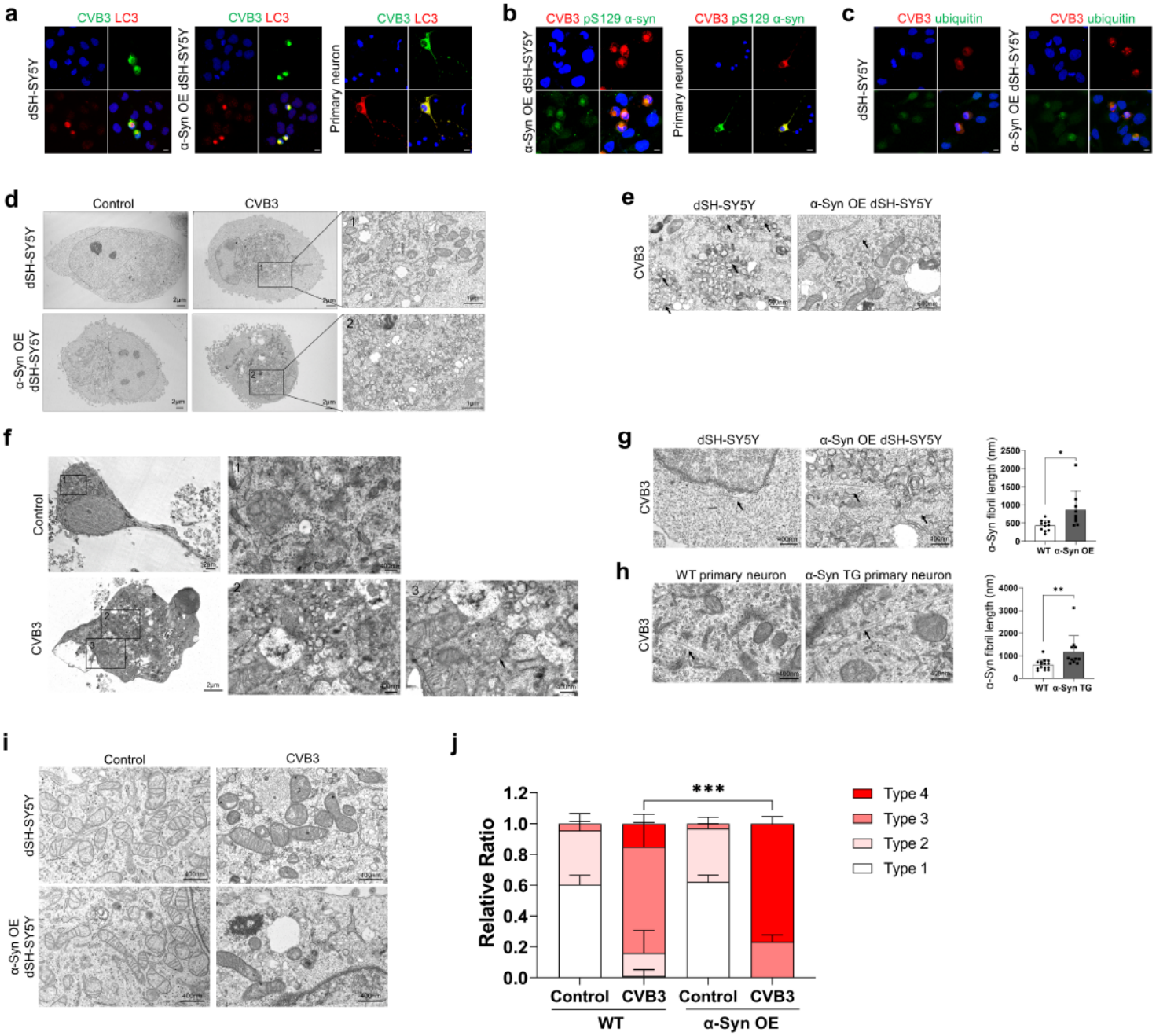

Figure 2

CVB3 infection induces Lewy body-like inclusion body formation in neurons. a Immunocytochemistry (ICC) images of WT, α-syn OE dSH-SY5Y cells and mouse primary cortical neurons infected by CVB3 for 24 h. CVB3 VP1 (green) and MAP1LC3B (LC3) (red) were immunostained. Images are representative of three independent experiments. b ICC images of α-syn OE dSH-SY5Y cells and mouse primary cortical neurons infected with CVB3. CVB3 VP1 (red) and pS129 α-syn (green) were immunostained. c ICC images of WT and α-syn OE dSH-SY5Y cells infected by CVB3. Colocalization of CVB3 VP1 (red) and ubiquitin (green) was observed. Images are representative of three independent experiments. Scale bar indicates 10 μm. Blue indicates DAPI. d Transmission electron microscopy image of control and CVB3 infected WT and α-syn OE dSH-SY5Y cells which were infected with CVB3. e TEM image of CVB3 infected WT and α-

syn OE dSH-SY5Y cells which were infected with CVB3. Arrows indicate viral particles. f TEM image of control and mouse primary cortical neurons infected by CVB3 for 24 h. Arrows indicate viral particles. g The length of α-syn fibrils between CVB3 infected WT and α-syn OE dSH-SY5Y was analyzed. Arrows indicate α-syn fibrils. *P < 0.05, unpaired t-test. h The length of α-syn fibrils between CVB3 infected WT and α-syn TG primary neuron was analyzed. Arrows indicate α-syn fibrils. **P < 0.01, unpaired t-test. i TEM image of control and CVB3 infected WT and α-syn OE dSH-SY5Y cells. j TEM analysis of mitochondrial types of WT and α-syn OE dSH-SY5Y cells infected with CVB3. *** P < 0.001, one-way ANOVA test with Tukey's multiple comparisons test. dSH-SY5Y SH and primary cortical neuron were infected with CVB3 of 0.25 and 5 MOI, respectively, for 24 hours. All images are representative of three or more independent experiments. All intensity values were also derived from three or more independent experiments.

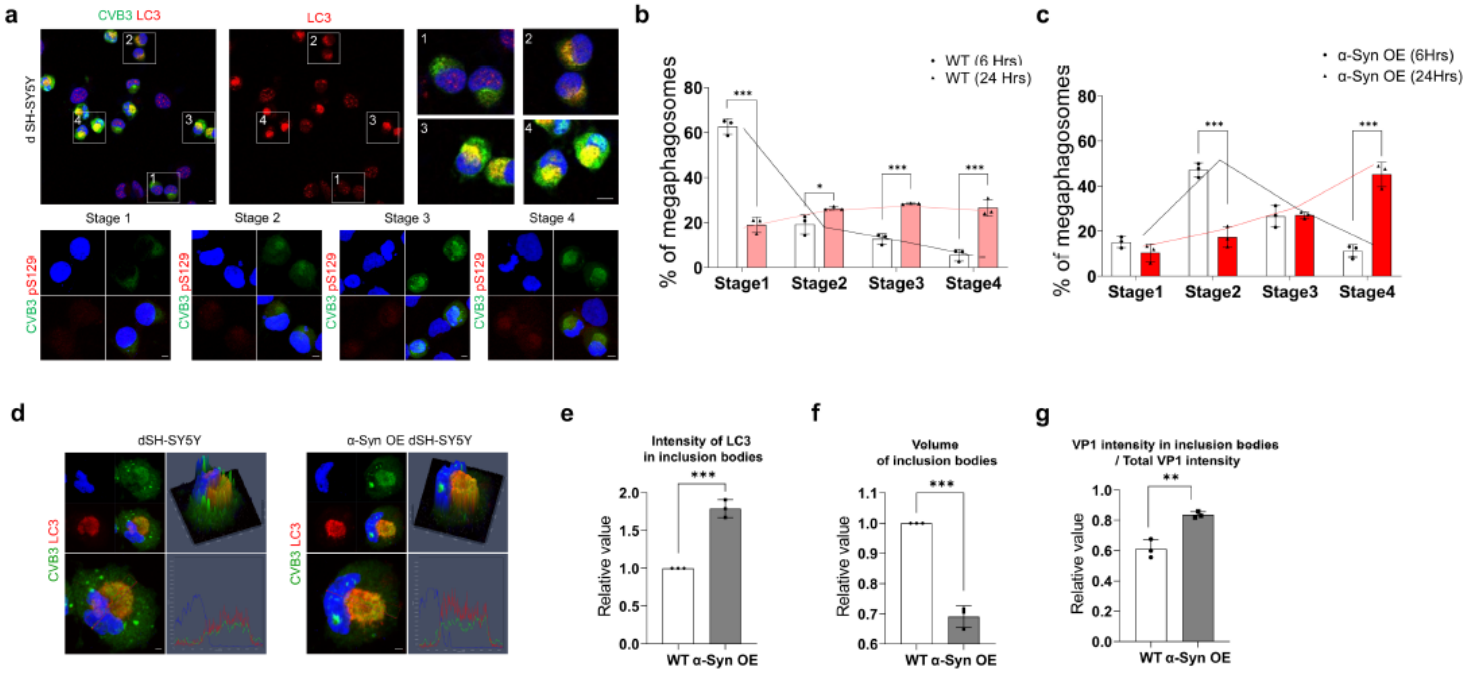

Figure 3

α-Syn regulates maturation of Lewy body-like inclusion bodies induced by CVB3. a Immunocytochemistry (ICC) image of dSH-SY5Y cells infected with CVB3 (MOI 0.25, here and hereafter) for 24 h. CVB3 VP1 (green) and MAP1LC3B (LC3) (red) was immunostained. Higher magnification of images enclosed in numbered white boxes indicates stages of inclusion bodies based on the staining patterns of LC3. CVB3 VP1 (green) and pS129 α-syn (red) were immunostained. Scale bar indicates 10 μm. Blue indicates DAPI. b ICC image analysis of the ratio of inclusion bodies in each stage in dSH-SY5Y cells infected with CVB3 for 6 and 24 h (n=3). *** P < 0.001, * P < 0.05, two-way ANOVA test with Sidak's multiple comparisons test. c ICC image analysis of the ratio of inclusion bodies in each stage of α-syn OE dSH-SY5Y cells infected with CVB3 for 6 and 24 h (n=3). *** P < 0.001, two-way ANOVA test with Sidak's multiple comparisons test. d ICC image of VP1 (green) and LC3 (red) colocalization patterns in WT and α-syn OE dSH-SY5Y cells infected with CVB3 for 24 h. Scale bar indicates 2 μm. Blue indicates DAPI. e-f ICC image analysis of the LC3 intensity and volume of inclusion bodies in each stage in WT and α-syn OE dSH-SY5Y

cells infected with CVB3 for 24 h (n=3). *** P < 0.001, ** P < 0.01, one-way ANOVA test with Tukey's multiple comparisons test. g ICC image intensity analysis of the VP1 in inclusion bodies per total VP1 intensity in each stage in WT and α-syn OE dSH-SY5Y cells that were infected with CVB3 for 24 h (n=3). *** P < 0.001, ** P < 0.01, * P < 0.05, one-way ANOVA test with Tukey's multiple comparisons test. All images are representative of three or more independent experiments. All intensity values were also derived from three or more independent experiments.

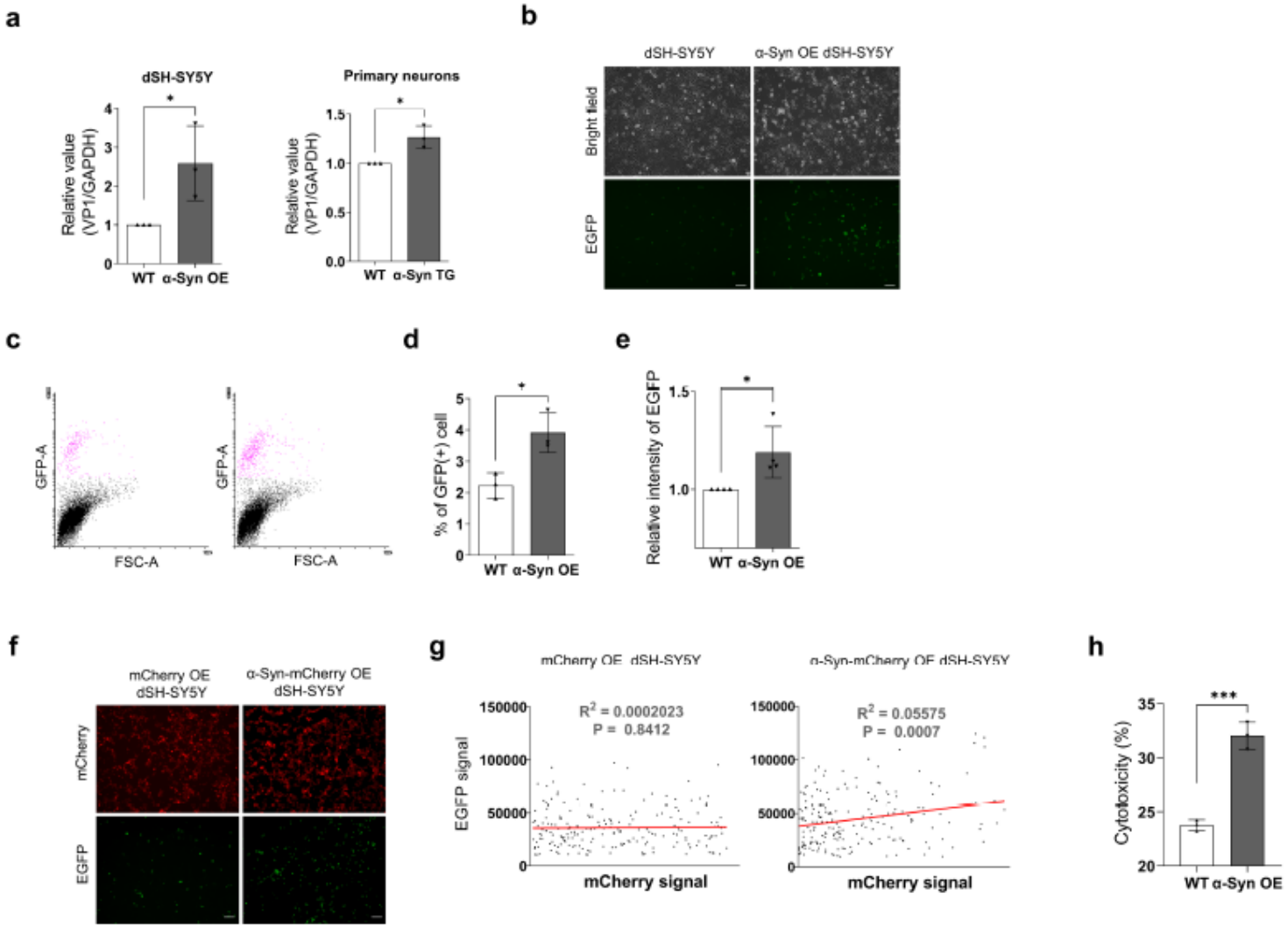

Figure 4

α-Syn regulates replication of CVB3 in neurons. a The relative level of VP1 between WT and α-syn OE dSH-SY5Y cells (0.25 MOI) or WT and α-syn TG mice primary cortical neurons (5 MOI) that were infected with CVB3 for 24 h. Values were derived from three independent experiments (n=3). * P < 0.05, unpaired t-test. b Fluorescence microscopic image of WT and α-syn OE dSH-SY5Y cells that were infected with 0.6 MOI CVB3 variant co-expressing EGFP (CVB3-EGFP) for 24 h. Scale bar indicates 50 μm. c-e Flow cytometric analysis was performed. The number of EGFP-positive cells (d) and the intensity (e) were analyzed using WT and α-syn OE dSH-SY5Y cells that were infected with 0.6 MOI CVB3-EGFP for 24 h (n=3 or 4). * P < 0.05, unpaired t-test. f Fluorescence microscopic images of mCherry and mCherry α-syn OE dSH-SY5Y cells infected with 0.6 MOI CVB3-EGFP for 24 h (n = 3). Scale bar indicates 50 μm. g Linear

regression analysis of mCherry and EGFP intensity of mCherry and α-syn-mCherry OE dSH-SY5Y cells infected with 0.6 MOI CVB3-EGFP for 24 h (n = 3). h Cytotoxicity analysis using lactate dehydrogenase assay of WT and α-syn OE dSH-SY5Y cells infected with 0.25 MOI CVB3 for 30 h (n=3). *** P < 0.001, unpaired t-test. All images are representative of three or more independent experiments. All intensity values were also derived from three or more independent experiments.

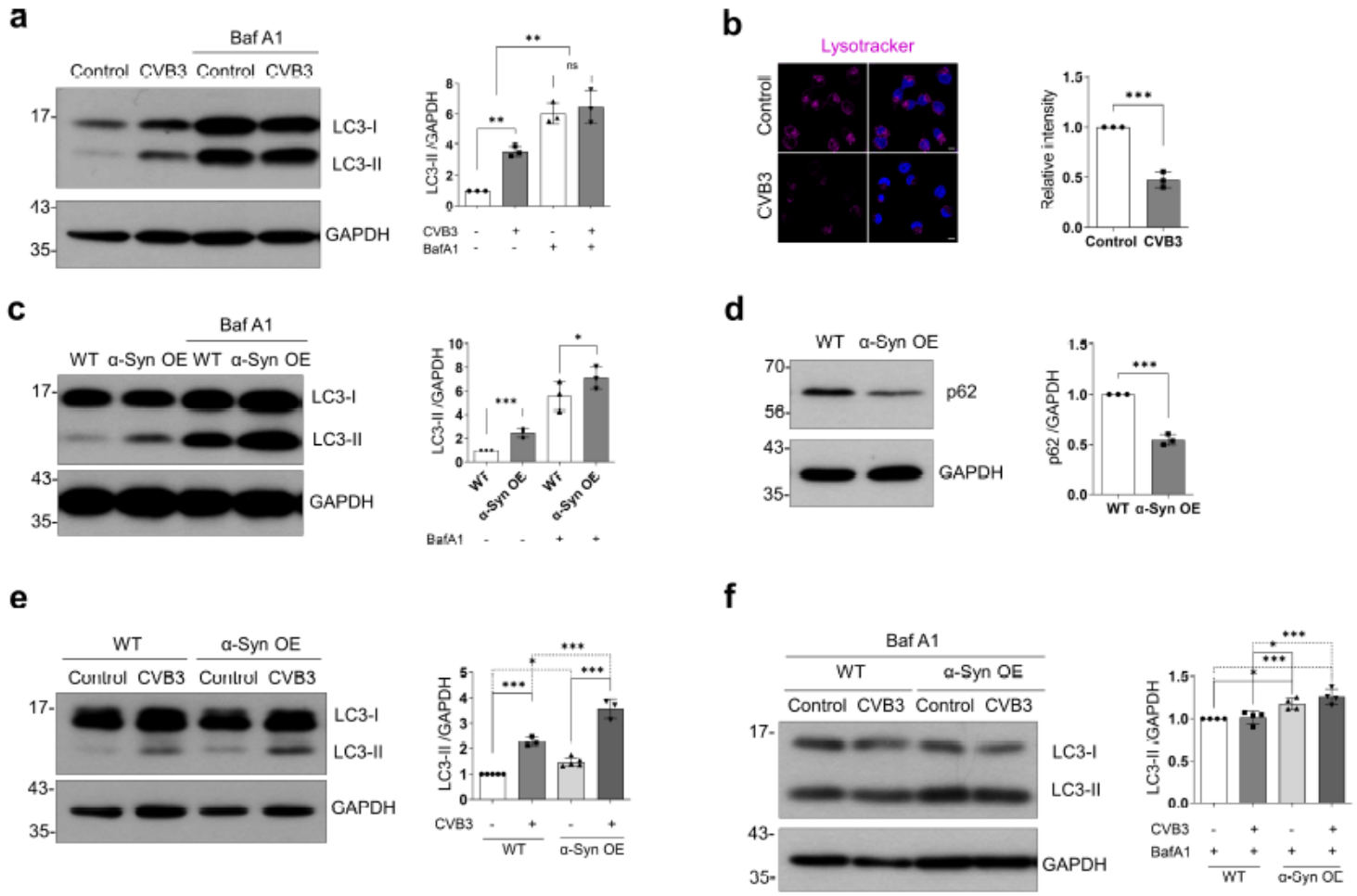

Figure 5

CVB3 and α-syn differentially regulate autophagic activity. a Samples of control and CVB3 infected (0.25 MOI for 24 h) dSH-SY5Y cells with dimethylsulfoxide (DMSO) or 50 nM bafilomycin A1 (BafA1) were lysed and western blot was performed with LC3 antibody. Protein levels were quantified by densitometry (n=3). b ICC image of dSH-SY5Y cells infected with 0.25 MOI CVB3 for 24 h. Fluorescence was seen using LysoTracker (n=3). Scale bar indicates 10 μm. c The relative level of LC3 expression between WT and α-syn OE dSH-SY5Y cells with DMSO or 50 nM BafA1. Protein levels were quantified by densitometry (n=3). d The relative level of p62 expression between WT and α-syn OE dSH-SY5Y cells. Protein levels were quantified by densitometry (n = 3). e-f The relative level of LC3 expression between WT (control and CVB3) and α-syn OE (control and CVB3) dSH-SY5Y cells with DMSO or 50 nM BafA1. Cells were infected with 0.25 MOI CVB3 for 24 h. Images are representative of independent experiments. Protein levels were quantified by densitometry (n=3). dSH-SY5Y cells were infected with CVB3 of 0.25 MOI for 24 hours. *p <

0.05, **p < 0.01, or ***p < 0.001 versus indicated groups. One-way ANOVA (a, c, e, f) with Tukey's post hoc test; unpaired t-test (b, d). All images are representative of three or more independent experiments. All intensity values were also derived from three or more independent experiments.

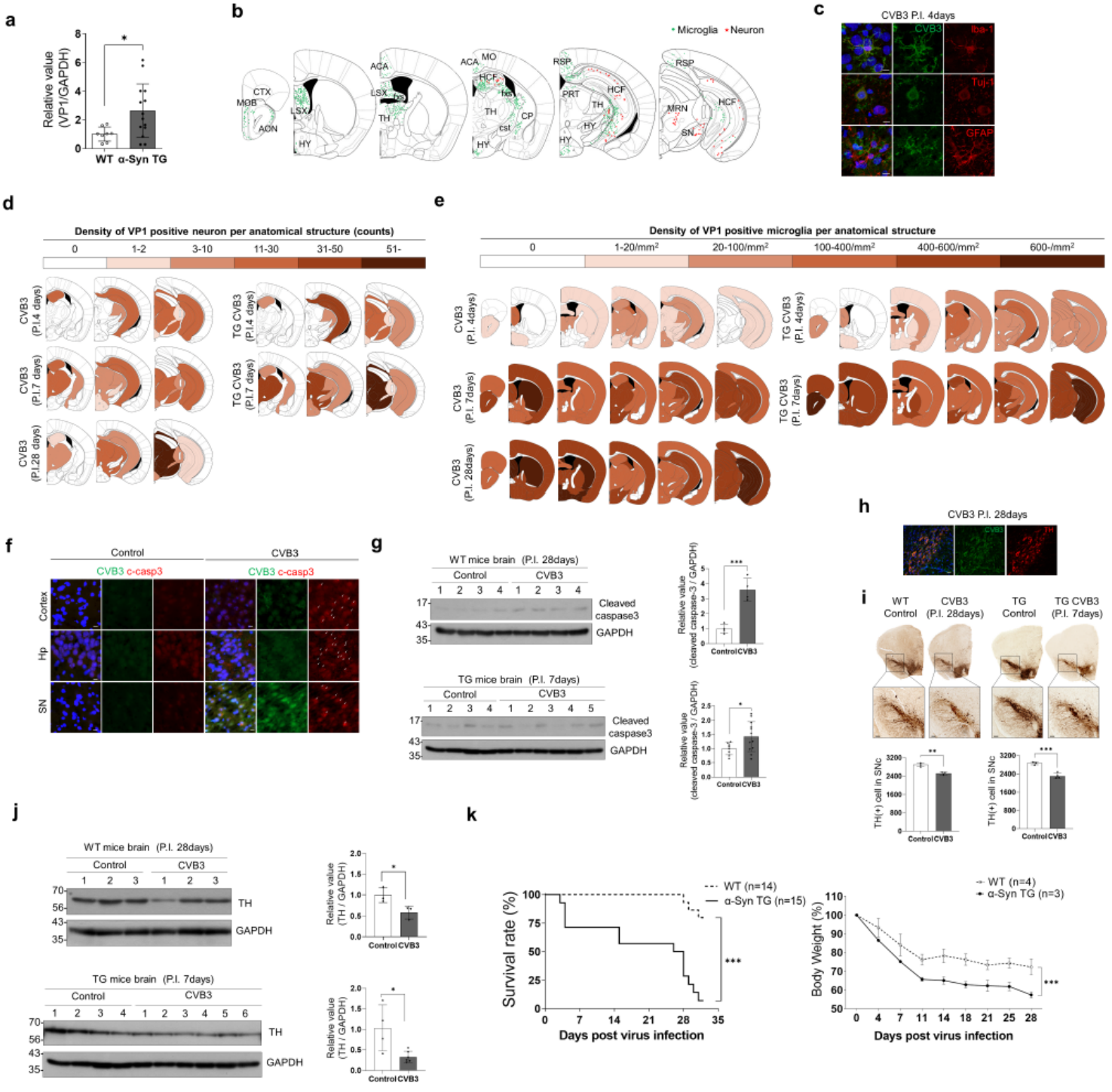

Figure 6

α-Syn regulates CVB3 replication in mouse brains. a The relative levels of VP1 between WT (n = 8) and α-syn TG (n = 14) mouse brain at day 7 postinfection (PI) of CVB3. b The localization of VP1 positive cells on immunohistochemistry (IHC) of mouse brain structure at day 4 PI. Microglia and neurons are evident

as green and red asterisks, respectively. (CTX-cortex, MOB-main olfactory bulb, AON-anterior olfactory nucleus, LSX-lateral septal complex, HY-hypothalamus, ACA-anterior cingulate area, fxs-fornix system, MO-somatomotor area, HCF-Hippocampal formation, TH-thalamus, CP-caudoputamen, Cst-corticospinal tract, RSP-retrosplenial area, PRT-pretectal region, MRN-midbrain reticular nucleus, SN-substantia nigra). c IHC image of CVB3 infected mice brain at day 4 PI. Colocalization of CVB3 VP1 with Iba-1, Tuj-1, and GFAP were observed. Scale bar indicates 10 μm. Blue indicates 4',6-diamidino-2-phenylindole (DAPI). d-e Time series (at day 4,7 and 28 PI) anatomic diagram illustrating the pattern of CVB3 infection. Tuj-1 (D) and Iba-1 (E) positive cell densities, which were colocalized with VP1 in CVB3 infected WT and α-syn TG mice were expressed in the corresponding color of the indicated number based on the anatomical structure. f IHC image of control and CVB3 infected mice brain at day 28 PI. Arrows indicate cleaved caspase3 positive cells. (Hp-hippocampus, SN-substantia nigra). Scale bar indicates 10 μm. Blue indicates DAPI. g Western blot was performed using control and CVB3 infected WT (at day 28 PI) and α-syn TG (at day 7 PI) mice. Protein levels were quantified by densitometry. h IHC image of CVB3 infected mice brain at day 28 PI. Colocalization of CVB3 VP1 with tyrosine hydroxylase (TH) was observed. Scale bar indicates 20 μm. Blue indicates DAPI. i TH-positive diaminobenzidine image of control and CVB3 infected mice brain at day 28 PI (WT) and at day 7 PI (α-syn TG). The number of TH-positive cells in the substantia nigra pars compacta (SNc) between control and CVB-infected mice were analyzed. Scale bar indicates 100 μm. j Western blot was performed using control and CVB3 infected WT (at day 28 PI) and α-syn TG (at day 7 PI) mice. Protein levels were quantified by densitometry. k Kaplan-Meier survival curves and body weight loss curve of CVB3 infected WT and α-syn TG mice. All mice were infected by intraperitoneal injection of 1.0 x 106 PFU of CVB3. *$p < 0.05$, **$p < 0.01$, or ***$p < 0.001$ versus indicated groups. unpaired t-test (a, g, i, j); Log-rank (Mantel-Cox) test (survival curve analysis), two-way ANOVA test (weight loss curve analysis).

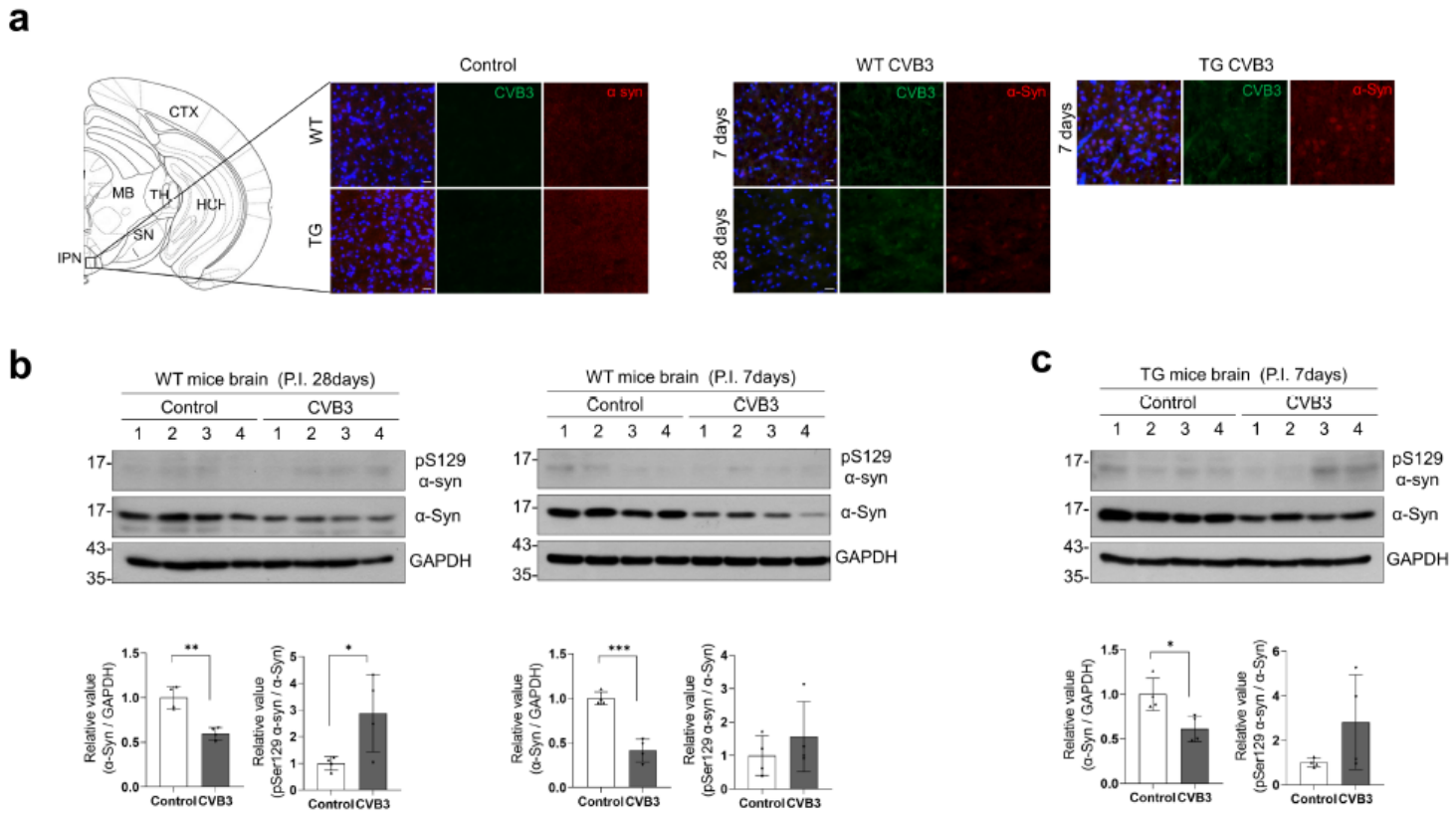

Figure 7

CVB3 induces α-syn inclusions in mouse brains. a Immunohistochemistry (IHC) image of control and CVB3 infected WT and α-syn TG mice brain at indicated dates PI. Scale bar indicates 20 μm. Blue indicates DAPI. (CTX-cortex, HCF-Hippocampal formation, MB-midbrain, TH-thalamus, SN-substantia nigra, IPN-interpeduncular nucleus). b-c Western blot was performed using control and CVB3 infected WT and α-syn TG mice brain at indicated dates PI. Protein levels were quantified by densitometry. *** P < 0.001, ** P < 0.01, * P < 0.05, unpaired t-test. All mice were infected by intraperitoneal injection of 1.0 x 106 PFU of CVB3.

Supplementary Files

This is a list of supplementary files associated with this preprint. Click to download.

- SupplementaryMaterial.pdf